Manuscript Number: JCR-D-15-01449R1

Title: Bacteriomimetic Invasin-Functionalized Nanocarriers for Intracellular Delivery

Article Type: Research paper

Keywords: Bacteriomimetic liposomes; bioinvasive carriers; intracellular delivery; cell uptake kinetics; receptor competition experiments

Corresponding Author: Dr. Hagar Ibrahim Labouta, Ph.D.

Corresponding Author's Institution: University of Calgary

First Author: Hagar Ibrahim Labouta, Ph.D.

Order of Authors: Hagar Ibrahim Labouta, Ph.D.; Sara Menina; Annika Kochut; Sarah Gordon; Rebecca Geyer; Petra Dersch; Claus-Michael Lehr

Abstract: Intracellular bacteria invade mammalian cells to establish an infectious niche. The current work models adhesion and subsequent internalization strategy of pathogenic bacteria into mammalian cells to design a bacteriomimetic bioinvasive delivery system. We report on the surface functionalization of liposomes with a C-terminal fragment of invasin (InvA497), an invasion factor in the outer membrane of Yersinia pseudotuberculosis. InvA497-functionalized liposomes adhere to mammalian epithelial HEp-2 cell line at different infection stages with a significantly higher efficiency than liposomes functionalized with bovine serum albumin. Covalent attachment of InvA497 results in higher cellular adhesion than liposomes with physically adsorbed InvA497 with non- specific surface protein alignment. Uptake studies in HEp-2 cells indicate active internalization of InvA497-functionalized liposomes via β1-integrin receptor-mediated uptake mechanism mimicking the natural invasion strategy of Yersinia pseudotuberculosis. Uptake studies in Caco-
2 cells at different polarization states demonstrate specific targeting of the InvA497-functionalized liposomes to less polarized cells reflecting the status of inflamed cells. Moreover, when loaded with the anti-infective agent gentamicin and applied to HEp-2 cells infected with Yersinia pseudotuberculosis, InvA497-functionalized liposomes are able to significantly reduce the infection load relative to non-functionalized drug-loaded liposomes. This indicates a promising application of such a bacteriomimetic system for drug delivery to intracellular compartments.

*Graphical Abstract

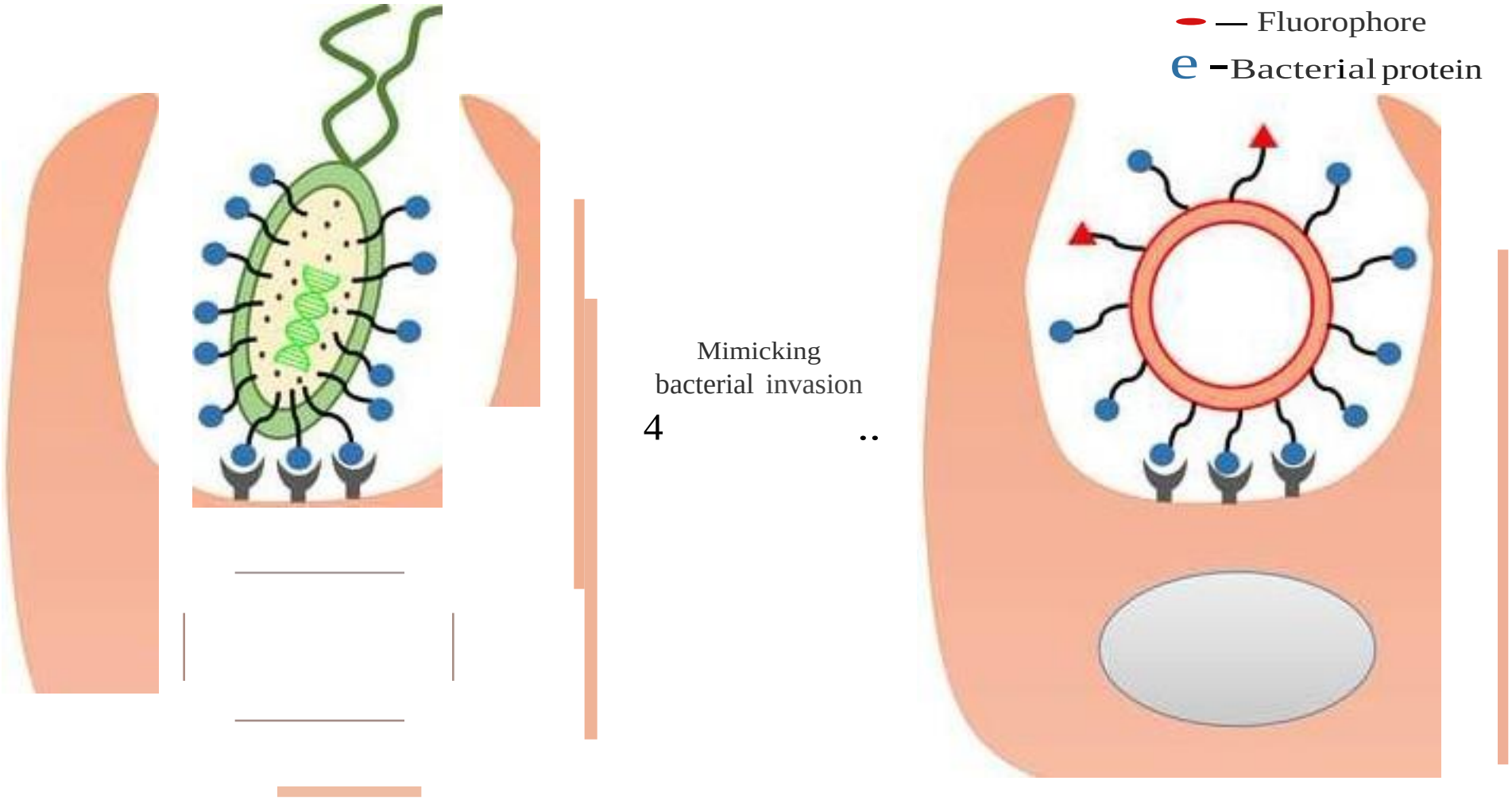

Bacterial invas on into a human cell via outer membrane proteins

Intracellu ar delivery of bacteriomimetic liposomes

Bacteriomimetic Invasin-Functionalized Nanocarriers for Intracellular Delivery

Hagar Ibrahim Labouta[1,2,†], *Sara Menina*[1], *Annika Kochut*[3], *Sarah Gordon*[1], *Rebecca Geyer*[3], *Petra Dersch*[3] *and Claus-Michael Lehr*[1,4,*]

[1]Dept. of Drug Delivery (DDEL), Helmholtz-Institute for Pharmaceutical Research Saarland (HIPS), Helmholtz Center for Infection Research (HZI), Campus A4 1, D-66123 Saarbrücken, Germany, [2]Department of Pharmaceutics, Alexandria University, Alexandria, 21521 Egypt, [3]Department of Molecular Infection Biology, Helmholtz Centre for Infection Research, 38124 Braunschweig, Germany, [4]Department of Pharmacy, Saarland University, D-66123 Saarbrücken, Germany.

*Corresponding author e-mail: Claus-Michael.Lehr@helmholtz-hzi.de

† Present Address: Department of Chemistry, Faculty of Science & Cellular and Molecular Bioengineering Research Laboratory (CMBRL), Schulich School of Engineering, University of Calgary, Calgary, Canada.

KEYWORDS: Bacteriomimetic liposomes; bioinvasive carriers; intracellular delivery; cell uptake kinetics; receptor competition experiments.

ABSTRACT

Intracellular bacteria invade mammalian cells to establish an infectious niche. The current work models adhesion and subsequent internalization strategy of pathogenic bacteria into mammalian cells to design a bacteriomimetic bioinvasive delivery system. We report on the surface functionalization of liposomes with a C-terminal fragment of invasin (InvA497), an invasion factor in the outer membrane of *Yersinia pseudotuberculosis*. InvA497-functionalized liposomes adhere to mammalian epithelial HEp-2 cell line at different infection stages with a significantly higher efficiency than liposomes functionalized with bovine serum albumin. Covalent attachment of InvA497 results in higher cellular adhesion than liposomes with physically adsorbed InvA497 with non-specific surface protein alignment. Uptake studies in HEp-2 cells indicate active internalization of InvA497-functionalized liposomes via β_1-integrin receptor-mediated uptake mechanism mimicking the natural invasion strategy of *Yersinia pseudotuberculosis*. Uptake studies in Caco-2 cells at different polarization states demonstrate specific targeting of the InvA497-functionalized liposomes to less polarized cells reflecting the status of inflamed cells. Moreover, when loaded with the anti-infective agent gentamicin and applied to HEp-2 cells infected with *Yersinia pseudotuberculosis*, InvA497-functionalized liposomes are able to significantly reduce the infection load relative to non-functionalized drug-loaded liposomes. This indicates a promising application of such a bacteriomimetic system for drug delivery to intracellular compartments.

1. Introduction

Functionalizing nanoparticles with peptide tags to initiate or enhance nanoparticles uptake by mammalian cells have significantly increased over the past years. Yet, impact on clinical praxis remains disappointing. One of the promising approaches, yet not much explored, is nanoparticle functionalization with bacterial outer membrane adhesins or invasins, i.e. proteins essential for cell adhesion and invasion of bacterial pathogens. Early trials indicate efficient cellular delivery using lectin [1, 2] and invasin (InvA497) [2-5] surface treated particles. This is the first in-depth mechanistic study investigating the cellular interaction of bacteriomimetic nanocarriers decorated with a truncated bacterial protein ligand in presence of the modeled bacterial counterpart.

Yersinia species (*Y. pseudotuberculosis* and *Y. enterocolitica*) are facultative intracellular pathogens that elaborate several surface bacterial ligands involved in virulence, one of which is invasin (InvA).[6, 7] InvA is an outer membrane protein required for the efficient cellular uptake of enteric *Yersinia* species by binding to members of the β_1-integrin receptor family (e.g. $\alpha_5\beta_1$). Integrins are heterodimeric integral membrane proteins mediating communication between the extracellular environment and the cytoskeleton by binding to cytoskeletal components and either extracellular matrix proteins or other cell surface proteins. InvA binding to β_1-integrins leads to a reorganization of the host cytoskeleton and formation of pseudopods that migrate around the bacteria and enclose them into a membrane-bound vacuole.[8] This study makes use of the detailed knowledge of the InvA-mediated cell adhesion and subsequent internalization of the Gram-negative bacterium *Y. pseudotuberculosis* to design a “bacteriomimetic” delivery system; InvA497-functionalized liposomes.

Early trials to enhance uptake into mammalian cells on coupling InvA to nanoparticles [1, 3-5, 9] and microparticles [10, 11] used polymers. However, modelling the bacterial flexibility and the

bacterial membrane structure, liposomal carriers hold more promise. Yet, from the delivery aspect, the impact of InvA functionalization on rather more physiologically compatible, easily loadable nanoparticulate systems for therapeutic applications remains to be shown. To the best of the authors' knowledge, this is the first study reporting the potential of bacteriomimetic liposomes functionalized with a C-terminal fragment of the InvA protein (Inv497) and their uptake mechanism and kinetics in comparison to their natural bacterial counterparts. The system invasion efficacy was challenged in presence of *Y. pseudotuberculosis*, the bacteria expressing InvA. As a proof of concept, the therapeutic effect of InvA497-functionalized liposomes was demonstrated when loaded with the hydrophilic and poorly permeable aminoglycoside antibiotic gentamicin as a model anti-infective. Gentamicin-loaded InvA497-functionalized liposomes were employed in a human epithelial cell model preinfected with an invasive *Y. pseudotuberculosis* serotype O:3 strain, and assessed for their ability to affect intracellular bacterial killing.

2. Experimental Section

2.1. Overexpression and Purification of the Cell-surface Exposed C-terminal Domain of Invasin (InvA497)

InvA497 was extracted and purified according to previous studies.[6] Two liters of *E. coli* BL21 expressing the His-tagged C-terminal 497 amino acids of InvA (His6-InvA497) from *Y. pseudotuberculosis* were grown at 37 °C in Luria broth medium (LB) (Carl Roth GmbH, Karlsruhe, Germany) to an A600 = 0.4. The culture temperature was then shifted to 17 °C and grown to an A_{600} = 0.6. Isopropyl-b-D-thiogalactopyranoside was added to a final concentration of 100 μM to induce the expression His6-InvA497. Cells were allowed to grow overnight at 17 °C, followed by washing in order to produce a cell pellet. The cell pellet was then resuspended in

50 ml cold lysis buffer containing 50 mM NaH_2PO4, 300 mM NaCl, 10 mM imidazole (pH 8) together with a protease inhibitor cocktail containing 5 mM phenylmethylsulfonyl fluoride, 10 mM pepstatin, 10 mM E64 protease inhibitor, 20 mM leupeptin and 10 mM chymostatin. The cells were disrupted using a french press (2x at 1000 psi). The His6-InvA497 protein was purified by affinity chromatography with Ni-NTA Agarose (Qiagen, Venlo, Limburg, The Netherlands), eluted in elution buffer containing 50 mM NaH_2PO_4, 300 mM NaCl and 250 mM imidazole (pH 8) and dialyzed twice against 10 mM Tris buffer (Trisaminomethane, pH 8) containing 300 mM NaCl. Protein concentrations were determined by the Bradford protein assay (Pierce, Rockford, IL, USA).

2.2. Preparation of Fluorescent Liposomes Containing Carboxylic groups

Liposomes were prepared by lipid film hydration followed by membrane extrusion to obtain monodispersed unilamellar vesicles following a previously published method after modification.[12] In detail, 1,2-dipalmitoyl-sn-glycero-3-phosphocholine (DPPC) (Lipoid GmbH, Ludwigshafen, Germany), cholesterol (Sigma-Aldrich, Steinheim, Germany) and 1,2-dihexadecanoyl-sn-glycero-3-phosphoethanolamine-N-(glutaryl) (sodium salt) (Avanti Polar Lipids, Inc., Alabaster, USA) in a molar ratio of 6:3:0.6 were dissolved in 5 ml chloroform-methanol mixture, 2:1. A 100 µl of 0.5 mg/ml choroformic solution of the fluorescent dye “1,2-dipalmitoyl-sn-glycero-3-phosphoethanolamine-N-(lissamine rhodamine B sulfonyl)

(ammonium salt)" (Avanti Polar Lipids, Inc., Alabaster, AL, USA) was added. The final lipid mixture (19.2 mM) was dried in a rotary evaporator (Büchi, Essen, Germany) at 70 °C, 200 mbar and 145 rpm for 1 h to form a thin uniform lipid film. Complete evaporation of the remaining solvents was achieved by further heating at the same temperature under a pressure of 40 mbar with 145 rpm for further 30 min. The lipid film was then hydrated with 5 ml 100 mM MES (4-Morpholineethanesulfonic acid) buffer, pH 6 at a speed of 55 rpm for 1 h at 50 °C. Unilamellar liposomes were prepared by extruding the resulting multilamellar vesicles through 200 nm polycarbonate membrane (AMD Manufacturing Inc., Ontario, Canada) at 60°C under high pressure using nitrogen flow in a sealed stainless steel jacketed extruder (liposoFast L-50, Avestin, Mannheim, Germany). Liposomal dispersions were diluted 1:10 with MES and stored at 4 °C prior to further use.

2.3. Liposome Surface Functionalization

Liposomes were surface functionalized with either InvA497 or bovine serum albumin (BSA; Sigma Aldrich, Steinheim, Germany). A volume of 2 ml liposomal dispersion was incubated overnight with 300 µl of crosslinking agent, consisting of 48 mM EDC/19 mM NHS (EDC: N-(3-dimethylaminopropyl)-N´-ethylcarbodiimide hydrochloride; Sigma Aldrich, Steinheim, Germany; NHS: N-hydroxysuccinimide 99 %; Carbolution Chemical GmbH, Saarbrücken, Germany) in MES buffer (pH6) with gental shaking at room temperature. Liposomes were centrifuged (Rotina 420R; Hettich Zentrifugen, Tuttlingen, Germany) in Centrisart® tubes 300,000 MWCO (Sartorius, Goettingen, Germany) at 3270 g, 4 °C for 30 min to remove excess free reagent followed by three successive washing steps during which the MES buffer was

gradually exchanged with phosphate buffer saline (PBS) (Sigma Aldrich, Steinheim, Germany), pH 7.4 . The total volume was then completed to 2.5 ml with PBS. A 300 µl volume of 1 mg/ml InvA497 or BSA in PBS was added and coating process was continued overnight in ice bath with gentle shaking. This was followed by centrifugation and washing steps in Centrisart® tubes 300,000 MWCO to remove unbound protein.

2.4. Measurement of Colloidal Characteristics

Liposomes, 0.2 µM, were characterized for mean diameter, polydispersity index (PDI) and zeta potential using the ZetaSizer Nano (Malvern Instruments Ltd., Malvern, UK) before and after covalent protein attachment. Colloidal stability of liposomes in biological media was also investigated. Measurements were performed in triplicates.

2.5. Determination of Protein Functionalization Efficiency

The amount of InvA497 or BSA coupled to the surface of liposomes was quantified using a bicinchoninic acid (BCA) kit, in accordance with the manufacturer's instructions (QuantiPro^{TM}; Sigma-Aldrich, Steinheim, Germany). This assay is suitable to measure even proteins covalently bound to surfaces.[13] Absorbance was measured at 562 nm and concentration was determined reference to preconstructed calibration curves of InvA497/BSA in the presence of control liposomes to correct for lipid interference. Protein quantification was also performed using SDS-PAGE and western blot following a protocol by Schulze et al.[14]

2.6. Cell Cultures and Treatments

The human epithelial type 2, HEp-2 cell line (CCL-23 ™; ATCC, Manassas, VA, USA) originating from a human laryngeal carcinoma and expressing the β_1 integrin receptor was cultivated in Roswell Park Memorial Institute medium (RPMI 1640) (Gibco by life technologies™, Paisley , UK) supplemented with 10 % fetal calf serum (FCS) (Lonza, Cologne, Germany) and kept in culture for a maximum of 2 months after thawing.

Caco-2 cells, clone C2Bbe1 (CRL-2102™; ATCC, Manassas, VA, USA) were cultivated in Dulbecco's modified Eagle's medium (DMEM) supplemented with 10 % FCS and 1 % non-essential amino acids (PAA cell culture company, Pasching, Austria) and used at passages 58-72.

2.7. Cell Viability Assay

An ATP bioluminescent assay (ViaLight™ Plus, Lonza, Basel, Switzerland) was used to determine the viability of both HEp-2 and Caco-2 cells in response to treatment with liposomal formulations. This assay is based on enzymatic determination of ATP present in all metabolically active cells. Luciferase enzyme is employed to catalyze the formation of light from ATP and luciferin, the emitted intensity of which is linearly related to the ATP concentration.[15] A volume of 100 µl of a series of 0.12-1.92 µM liposomal dispersions was tested on confluent HEp-2 cells, and confluent and 50 % confluent Caco-2 cells seeded in 96-well plates (Greiner bio-one, Frickenhausen, Germany). InvA497-functionalized and non-modified liposomes were tested in parallel. HEp-2 and Caco-2 cells were incubated with the liposomes for 4 and 8 h, respectively. Cell lysis reagent®, 50 µl/well, was added to extract ATP from the cells. A volume

of 100 µl of each of the cell lysate and ATP monitoring reagent Plus® were incubated in 96-well white walled luminometer plate (Optiplate™-96; PerkinElmer Inc., Waltham, MA, USA) for 2 min at room temperature in the dark. Bioluminescence was measured (Tecan Deutschland GmbH, Crailsheim, Germany). Cells grown in culture medium only were considered as negative control (100 % cell viability) and others incubated with Triton X-100 (2 % w/v) were used as positive control (0 % cell viability). Percentage cell viability was calculated based on five replicates as shown in Equation 1.

$$Cell\ viability\ (\%) = \frac{Lum_{exp} - Lum_{negative\ control}}{Lum_{negative\ control} - Lum_{positive\ control}} \times 100 \quad (1)$$

In parallel, ATP controls in concentrations of 1.5 and 0.015 µM were prepared. A 50 µl volume of each of the control and the liposomes was incubated together with 100 µl ATP monitoring reagent Plus® and bioluminescence was measured to check for wavelength interference in absence of cells.

2.8. Cell-adhesion Experiments

Cell adhesion of InvA497-functionalized liposomes versus liposomes with physically adsorbed InvA497 was tested. Amount of physically adsorbed protein was equivalent to covalently coupled protein as determined by Bradford assay (Thermo Scientific, MA, USA). Appropriate control liposomes were also employed in parallel; BSA-functionalized liposomes and liposomes with physically-adsorbed BSA.

One day prior to adhesion experiments, HEp-2 cells were seeded in 8 well µ-slides (Ibidi, Martinsried, Germany) at a density of $1x10^4$ cells/well. Concomitantly, constitutively GFP-

expressing *Y. pseudotuberculosis* was cultivated in LB medium (lysogeny broth, Carl Roth GmbH, Karlsruhe, Germany).

Three sets of adhesion experiments were performed in parallel, at a temperature of 25 °C. In the first set of experiments a late stage of infection was simulated - cells were infected with bacteria (50 μl of $1x10^6$ bacteria/well) 30 min before addition of 50 μl/well of liposomes. In the second experimental set, simulating an early infection stage, both bacteria and liposomes were applied to cells simultaneously. For the third experimental set, simulating the healthy state, liposomes were applied to cells in absence of any bacterial treatment. Subsequently, cells were washed three times with PBS and incubated in binding buffer (RPMI 1640 medium supplemented with 20 mM of HEPES (4-(2-hydroxyethyl)-1-piperazineethanesulfonic acid, pH 7) and 0.4 % BSA) before addition of bacteria and/or liposomes. Cells were incubated for 1 h with test liposomes at a concentration of $4x10^4$ liposomes/ml, after which culture medium was removed and cells were washed three times with PBS. Cells were then fixed using 4 % paraformaldehyde in PBS for 10 min, and blocked and permeabilized by incubation with blocking buffer (5 % goat serum, 0.1 % Triton X-100 in PBS) for 60 min. Cell nuclei were stained by DAPI (4',6-diamidino-2-phenylindole, Carl Roth, Karlsruhe, Germany).

Cell adhesion was examined using fluorescence microscopy (Zeiss Axioskope; Zeiss, Jena, Germany) followed by image analysis by the freeware ImageJ (http://rsbweb.nih.gov/ij/). Image analysis was based on a previously established method in which the number of pixels due to liposomal fluorescence was calculated. The number of liposomes was estimated based on the area of a single diffraction-limited fluorescent spot; $\pi(rxy)^2$ (Equation 2),[16-18] 0.359 μm^2 in this study based on λ (emission wavelength for rhodamine) = 564nm and NA (numerical aperture of the optical lens) = 1.1.

$$r_{xy} = \frac{0.7\lambda}{NA} \quad (2)$$

2.9. Cell Uptake Studies

In preparation for uptake assays, InvA497-functionalized and control non-modified liposomes (1.92 μM) were centrifuged at 20000 g for 30 min at 4 °C, redispersed in culture medium and sterilized upon filtration through 0.2 μm membrane filters (Sartorius Stedim Biotech GmbH, Goettingen, Germany). Cells previously seeded in 24-well imaging plates (Zell-Kontakt, Nörten-Hardenberg, Germany) to approximately 80 %, and 50 or 90 % confluency for HEp-2 and Caco-2 cells, respectively, were washed with PBS in order to remove culture medium.

2.9.1. Relative Liposomal Uptake

HEp-2 and Caco-2 cells were exposed to liposomes (500 μl/well) for 1, 4 or 8 h at 37 °C, 5 % CO_2. Following incubation, cells were washed with PBS and fixed with 4 % paraformaldehyde. Cells were then stained with fluorescein wheat germ agglutinin (Flu-WGA, 6.25 μg/ml, Vector Laboratories, Burlingame, CA, USA) and DAPI (6.66 ng/ml) in order to allow for visualization of cell membranes and cell nuclei, respectively. Imaging plates were protected from light and stored at 4 °C until analysis via fluorescence imaging, which was performed using an inverted confocal-multiphoton laser scanning microscope (ZEISS LSM 510 META, Carl Zeiss, Jena, Germany). The objective used was a water immersion lens 40 x (NA=1.1). Wavelengths of 543 nm, 488 nm and 720 nm were used for excitation of rhodamine-labelled liposomes, Flu-WGA-labeled cell membranes and DAPI-labeled nuclei, respectively. Z-stacks of cells were taken with

step sizes of 0.8 μm, and with optical scans of an area of 0.22 x 0.22 μm^2. The gain settings were adjusted for each measurement individually. For each captured z-stack, optical layers incorporating cell-internalized liposomes were chosen and a z-projection image of the red channel (red fluorescence due to liposomes) was developed using ImageJ. The number of pixels was computed and converted into weighted number of liposomes as described previously [16, 17] and as briefly referred to in the methodology of the adhesion experiments.

2.9.2. Liposomal Uptake Kinetics

In addition to analysis of uptake using fixed cells, live cell imaging was also undertaken in order to obtain further information regarding the kinetics of liposomal internalization. HEp-2 cells were seeded in 8-well μ-slides to about 80 % confluency, washed with cell culture medium, stained with Flu-WGA (6.25 μg/ml) for 5 min at 37 °C to facilitate cell membrane visualization, and washed again before liposomal application. μ-slides were transferred into an incubation chamber of the confocal microscope with a constant temperature of 37 °C and 5 % CO_2 level to maintain cell viability throughout the experiment. An area of interest was then selected and imaging was performed using the same settings as indicated above, with the exception of the optical image area which in this case was 0.27 x 0.27 μm^2. Z-stacks were sequestered at different time intervals (1, 2, 3 and 4 h). The thickness of the optical layer was kept as 0.8 μm. ImageJ was used to develop z-projection images of the red channel of the optical layers in the captured z-stacks followed by pixel analysis. The weighed number of liposomes was plotted versus time to determine cell uptake kinetics. To get more information on uptake kinetics within the first hour of liposome application, cell uptake experiments with 10 and 30 min incubation periods were conducted using the same set-up; however in this case cells were fixed before imaging as

described above, in order to avoid possible photobleaching-associated inaccuracies resulting from continuous laser exposure of the treated cells on Z-sectioning.

2.9.3. Mechanistic Uptake Studies

In order to assess the mechanism of liposomal uptake into HEp-2 cells, experiments were conducted at 37 °C or 4 °C for a period of 4 h. An additional set of mechanistic studies were also carried out in which cells were incubated with the potential uptake inhibitors anti-integrin β_1-antibody (1:100 dilution), NPC-15437 dihydrochloride, monoclonal anti-CD29 (Sigma Aldrich, Steinheim, Germany) (1 μM) and Akt inhibitor VIII (Calbiochem, San Diego, CA, USA) (25 μM) for 1 h at 37 °C before washing, liposome addition, and a further 4 h incubation. All inhibitors were dispersed in RPMI supplemented with 20 mM HEPES buffer (pH 7) and 0.4 % BSA. Cells were then prepared for analysis (washing, fixing and staining) and visualized using fluorescence imaging as described above for relative liposomal uptake studies.

2.10. Determination of Anti-infective Efficacy

In order to assess the ability of the bacteriomimetic carrier to function as an effective intracellular delivery system, InvA497-functionalized liposomes were loaded with the poorly permeable anti-infective gentamicin, characterized for colloidal properties and the amount of entrapped drug, and finally applied to an infected epithelial cell model.
Gentamicin-loaded liposomes were prepared by hydrating the lipid films (described earlier in the methodology followed to prepare drug-free liposomes) with 5 ml of gentamicin solution (10

mg/ml in PBS). This was followed by surface functionalization with InvA497. The incubation time with the crosslinking agent (EDC/NHS) was limited to 3 h to reduce the possibility of drug release overnight. The amount of gentamicin entrapped within liposomes was quantified using an O-phthaldialdehyde-(OPA) based fluorometric assay (Sigma-Aldrich, Steinheim, Germany) subsequent to a lipid extraction, as previously described.[19] The fluorescence of extracted samples was measured in a plate reader (Genios Pro, Tecan, Germany) with an excitation wavelength of 344 nm and an emission wavelength of 450 nm. The amount of gentamicin entrapped within liposomes was then calculated with reference to the fluorescence intensity of standard gentamicin solutions.

An *in vitro* killing assay was conducted using epithelial cells of the β_1 integrin receptor-expressing HEp-2 cell line. Cells were infected with an invasive *Y. pseudotuberculosis* serotype O:3 strain. For this, the culture medium of HEp-2 cells (previously seeded one day before the experiment in a 24 well-plate) was exchanged with binding buffer containing *Y. pseudotuberculosis* at 1:25 multiplicities of infection. Cell culture plates were then centrifuged at 6708 g for 5 min (Eppendorf 5810 R Centrifuge, Hamburg, Germany) to sediment bacteria onto the cells. Cells and bacteria were then incubated for 1 h at 37 °C and 5 % CO_2 to allow for binding and penetration of the bacteria into the cells. A 1 h-cell incubation with 50 µg/ml of free gentamicin in binding buffer was a key step in order to kill any remaining extracellular bacteria. Infected cells were then washed twice with PBS to eliminate both gentamicin and killed extracellular bacteria, leaving HEp-2 cells containing intracellular *Y. pseudotuberculosis*. Infected cells were then treated for 2 h with gentamicin-loaded liposomes functionalized with InvA497 (I-GL) containing 50 µg/ml gentamicin. Drug-free liposomes (1.3 mM); both non-modified (L) and InvA497-functionalized drug-free liposomes (I-L), and gentamicin loaded

liposomes (GL) containing 50 μg/ml gentamicin served as control formulations. Following liposomal treatment, infected cells were washed twice with PBS and lysed with 200 μl lysis buffer containing 0.1% Triton X-100. Remaining intracellular bacteria following liposomal incubation were quantified after plating cell lysates on LB plates for 48 h at 25 °C. Results were expressed as a percentage of bacterial killing relative to untreated cells (blank, B). ANOVA followed by Post-hoc analysis were performed to determine the statistical significance of observed differences. Differences were considered to be significant (*) at a *P*-value < 0.05.

3. Results and Discussion

3.1. Physico-chemical characteristics of liposome formulations

Monodisperse phospholipid fluorescent liposomes containing carboxylic groups were prepared by lipid film hydration method. Cholesterol in the bilayer was incorporated as a membrane stabilizer increasing the glass transition temperature.[20, 21]

To decorate the liposomal surface we used a C-terminal fragment of the InvA protein (InvA497) of *Y. pseudotuberculosis* an important protein which is required for efficient invasion of this bacterium into human cells.[8] A prerequisite for binding to the integrin $\alpha_5\beta_1$-receptor is that the C-terminal carboxylic group of InvA497 remains free, non-substituted and directed towards the outer part of the protein corona.[8] This was achieved via a two-step surface functionalization of liposomes in which the carboxylic groups on the liposomal surface were first activated by EDC/NHS mixture. EDC reacts with the carboxylic group, forming an amine-reactive O-acylisourea intermediate which subsequently reacts with an amine group forming an amide bond.

However, the O-acylisourea intermediate is very unstable and susceptible to hydrolysis resulting in low coupling efficiency. The addition of sulfo-NHS stabilizes the intermediate by converting it to a semi-stable amine-reactive NHS ester, thereby increasing the coupling efficiency.[22-24] In the second step, after washing off excess of non-covalently bound EDC, activated carboxylic groups on the liposomes react with the N-terminus of the surface-exposed InvA497 domain leaving the C-terminus of the adhesion molecule free for the interaction with the β_1-integrin receptors. This two-step procedure of protein coupling avoided loss of InvA497 activity as well as interprotein conjugation leading to protein supramolecules or even aggregates.[24] Liposomes were functionalized with InvA497 or BSA without any observed aggregation. Results of particle characterization are shown in Table 1. Size diameter of liposomes was around 143 nm. The zeta potential was in the range of -20 to -43 mV. Liposomes were found stable on overnight incubation in culture media at 37 °C with a PDI of approximately 0.05. Increase in zeta potential was observed upon protein coating indicating higher stability due to steric hindrance by the protein corona. The protein coating efficiencies determined by surface protein quantification using BCA and western blot assays were found comparable (Table 1).

3.2. Cell viability study

For the cell-liposomes association experiments, it was important to ensure that cell adhesion and uptake measured is induced by non-cytotoxic concentrations of liposomes. Furthermore, for biomedical purposes, especially for clinical applications, toxicity is a critical factor in the evaluation of their potential.[25] As the InvA497-functionalized liposomes are intentionally engineered to interact with and invade the cells, it is important to ensure that this

functionalization is not causing any cytotoxic effect. First, potential nanoparticle-dye interferences must be considered to avoid false-positive and false-negative results.[26, 27] No interference was observed measuring luminescence of ATP standards in the presence of liposomes (Figure S1). Figure 1 shows the viability of HEp-2 and Caco-2 cells after incubation with uncoated as well as InvA497-functionalized liposomes. No significant difference in cell viability was observed for non-modified liposomes or InvA497-functionalized liposomes compared to non-treated control cells, indicating that InvA497-functionalized liposomes are suitable and efficient drug delivery tools. The increased mean viability of cells after liposome exposure (Figure 1) could be due to cell proliferation over time in presence of phospholipids and cholesterol naturally present in cell membranes of mammalian cells.[28] Although only the small C-terminal portion of InvA is used for liposome coating, we cannot fully exclude immunostimulatory reactions via the production of inflammatory cytokines [29] and future tests are required to study the effects of the particles on the human immune system.

3.3. Cell-adhesion experiments: InvA497-functionalized liposomes promote tight adhesion to human epithelial cells

Challenging experiments were designed to investigate the ability of InvA497-functionalized liposomes to adhere to β_1-integrin expressing HEp-2 cells in the presence of InvA-expressing *Y. pseudotuberculosis*. Such studies were carried out at a temperature of 25 °C, conditions under which cell adhesion but no InvA-mediated invasion into host cells was observed.[2, 5] Liposome formulations with covalently-coupled InvA497 or BSA (as a negative control, non-invasive protein) were employed; in addition, liposomes with surface-adsorbed InvA497 and BSA were

used. Three different experimental sets were performed in which (i) only InvA497- or BSA-coated liposomes were added to HEp-2 cells in total absence of *Y. pseudotuberculosis* (healthy state), (ii) in which the liposomes were added simultaneously with InvA-expressing *Y. pseudotuberculosis* (mimicking early stage infection conditions), and (iii) in which the liposomes were added after infection with InvA-expressing *Y. pseudotuberculosis* (representing a late infection stage).

Liposomes with either physically adsorbed or covalently-linked surface BSA did not show significant adhesion to HEp-2 cells shown by fluorescence imaging (Figure 2a,b) and by calculating the number of cell-associated liposomes (Figure 2c). InvA497 functionalization resulted in significantly higher levels of cellular adhesion. Only 2-5 fold more cell-associated liposomes were observed with physically adsorbed InvA497-coated liposomes, while liposomes with covalently linked InvA497 resulted in a 32-38 fold increase in adhesion to HEp-2 cells relative to control liposomes covalently-linked with BSA (Figure 2c). This difference can likely be attributed to an optimal orientation of InvA497 in this formulation which allows the projection of the C-terminal region of InvA from liposomal surfaces facilitating integrin receptor-mediated adhesion (refer to Section 2.1), and testifies the successful design of a bioinvasive carrier with bacteriomimetic traits.

With respect to cell adhesion of liposomal formulations in simulated healthy, early or late infection stages, it was seen that simultaneous or pre-exposure of HEp-2 cells to the InvA-expressing bacterium *Y. pseudotuberculosis* led to a reduction in adhesion of InvA497 liposome formulations relative to adhesion under sterile conditions. This demonstrates that InvA497-modified liposomes compete with InvA-expressing bacteria for β_1-integrin-mediated cell adhesion (and eventually invasion). The fact that measurable levels of liposomal adhesion were

still noted even following pre-incubation of HEp-2 cells with InvA-expressing bacteria is however an encouraging observation. This suggests that these bacteriomimetic carrier can not only be used for intracellular delivery of anti-infective compounds as a prophylactic or early infection stage measure, but also as therapy of established intracellular infections which may be initiated by the identical adhesion/invasion mechanism.

3.4. Cell uptake kinetics and internalization mechanism into HEp-2 cells

Next, we determined the capacity of covalent InvA497-functionalization (as the optimal noted method of InvA497 attachment) to promote invasion/uptake of liposomes into HEp-2 cells and studied the uptake kinetics and the molecular internalization mechanism of InvA497-functionalized liposome uptake.

Cellular uptake of InvA497-functionalized liposomes was compared to that of both non-modified liposomes and BSA-functionalized liposomes as control formulations 1 and 4 h after application of the liposomes to HEp-2 cells. Knowing that the recycling time of $\alpha_5\beta_1$ integrin is 30 min [30], the chosen time frame is appropriate covering several receptor cycles. Yet, the incubation time is considered short enough to minimize non-specific uptake of cells through fluid-phase endocytosis [31]. More importantly, a time frame of 4 h was chosen according to the internalization timeline of *Y. pseudotuberculosis* into HEp-2 cells [32]; whereas most cell-attached bacteria are internalized after 4 h.

Representative confocal-multiphoton images are shown in Figure 3a and results of image analysis of the sequestered z-stacks are given in Figure 3b. Minimal induced cell uptake was observed for control liposomes likely resulting from non-receptor-mediated fusion of liposomal

and HEp-2 cell membranes.[33] Cell uptake was induced upon InvA497 coupling and the number of intracellular liposomes increased significantly over time.

To determine uptake kinetics, cell uptake into living HEp-2 cells was tracked over 4 h (Figure 4a). As the previously conducted fixed time point experiments demonstrated no difference in uptake between non-modified and BSA-functionalized liposomes (Figure 3), only non-modified liposomes were employed as the sole control formulation in all the following experiments. Z-projection images clearly showed that both non-modified and InvA497-functionalized liposomes accumulated within living cells over time, whereby the overall signal obtained for the InvA497-functionalized liposomes was significantly higher at each time point. (Figure 4a). In order to determine numbers of internalized liposomes, a pixel analysis of live cell images, as well as of cell samples incubated with liposomes for periods of 10 and 30 min followed by cell fixation (in order to avoid photobleaching and imaging inaccuracies resulting from continuous laser exposure on Z-sectioning) was conducted (Figure 4b). This analysis demonstrated that the overall number of internalized Inv497-coated liposomes was significantly higher at each time point compared to the controls. Moreover, the average uptake rate of InvA497-functionalized liposomes (507 liposomes/h) was approximately 7-fold higher relative to the control lipsomes (70 liposomes/h) (Figure 4b). Further analysis of the uptake profile of InvA497-functionalized liposomes showed that the InvA497-mediated uptake can be divided into three distinct phases: (i) an initial, exponential phase describing a rapid receptor-mediated internalization of liposomes; (ii) a plateau, typically indicative of saturation of uptake-mediating receptors [34]; followed by (iii) a linear uptake process characterized by a linear uptake rate.

To further characterize the uptake mechanism, HEp-2 cells were incubated with InvA497-functionalized and control liposomes at 4 °C and 37 °C to determine relative liposomal uptake

(Figure 5a). At 4 °C, energy-dependent uptake (e.g. endocytosis) is generally greatly reduced.[35] In fact, a significantly higher number of intracellular Inv497-coated liposomes were detectable at 37°C compared to 4°C, whereas no significant difference in cell uptake was observed with control liposomes (Figure 5a). This indicates that Inv497-functionalized liposomes are internalized by a receptor-specific uptake process. However, a minor extent of cell uptake of InvA497-functionalized liposomes appears to interact with the cell membrane non-specifically and facilitates uptake by some energy-independent processes, as shown by experiments done at 4°C (Figure 5a).

Finally, to verify that the cell uptake mechanism of InvA497-functionalized liposomes is receptor-specific and β_1-integrin-mediated, cell uptake inhibition experiments were conducted. In the first instance, anti-integrin β_1-antibody was incubated with HEp-2 cells before the addition of InvA497-functionalized liposomes. As shown in Figure 5b, a significant reduction in liposome uptake was observed in the presence of the anti-integrin β_1-antibody, indicating that uptake of InvA497-functionalized 497 occurs via β_1-integrin receptors [6]. Two inhibitors reported to reduce the InvA-triggered cell uptake of *Y. pseudotuberculosis*, Akt inhibitor VIII and protein kinase C (PKC) inhibitor NPC-15437,[32, 36] were employed to prove β_1-integrin-mediated liposome uptake. The serine/threonine kinase Akt and PKC are activated in response to many β_1-integrin-initiated signaling processes, including InvA-mediated uptake of *Y. pseudotuberculosis*.[36] Inhibition of either Akt or PKC resulted in a significant reduction in InvA497-functionalized liposomal cell entry, confirming their β_1-integrin-mediated uptake (Figure 5b). Application of the selective inhibitors reduced cell uptake to 22-29 %, similar to what has been shown for InvA-mediated uptake of *Y. pseudotuberculosis*.[36] This clearly

demonstrates that Inv497-coated liposomes enter via β_1-integrin-mediated uptake and verifies bacteriomimetitic characteristics of the developed InvA497-functionalized carrier.

3.5. Potential applications of bacteriomimetic nanocarriers in simulated states of inflammation and infection

3.5.1. Targeting Inflamed β_1-integrin Expressing Intestinal Mammalian Cells: Non-polarized versus Polarized Caco-2 cells

With particular respect to the human intestinal epithelium, it has been demonstrated that invasion by InvA-expressing *Y. pseudotuberculosis* occurs exclusively via interaction with β_1-integrins found on Microfold (M) cells,[37] as such receptors are not expressed on the apical side of differentiated polarized enterocytes.[38] However, under specific conditions (e.g. during intestinal inflammatory bowel disease or a bacterial infection) tight junctions open and β_1-integrins become more accessible on the apical surface of the enterocytes.[39] Knowing that Caco-2 cell line is a well-established model for the human intestinal barrier [40, 41], uptake into non-polarized and polarized Caco-2 cells was investigated in order to mimic the receptor distribution pattern in inflamed and healthy enterocytes, respectively. Cells at 50 % confluency express β_1-integrins on their apical surface (resembling the inflamed state), whereas cells grown to over 90 % confluency reduce the expression of the InvA receptor on the apical side according to the healthy state.[42] Application of InvA497-functionalized liposomes was seen to result in uptake only in the case of sub-confluent Caco-2 cells (Figure 6). Some adhesion of InvA-functionalized liposomes on polarized cells was also observed, however, this weak attachment was not sufficient to promote liposomal internalization. No uptake of the control liposomes was

observed regardless of the Caco-2 cell confluency level, demonstrating a clear advantage of the InvA497-functionalized system in to less-confluent enterocytes mimicking the inflamed state. The data suggest that InvA-mediated targeting of the β_1-integrin receptors could be exploited to develop drug delivery carriers targeting the inflamed intestinal epithelium.

3.5.2. Anti-infective Efficacy Studies

The ability of such a bacteriomimetic concept to facilitate effective intracellular delivery of the poorly permeable anti-infective agent gentamicin was investigated. For this purpose, HEp-2 cells infected with an invasive *Y. pseudotuberculosis* serotype O:3 strain [43-45] were employed. Infected HEp-2 cells were treated with gentamicin-loaded liposomes (GL), or gentamicin-loaded liposomes surface functionalized with InvA497 (I-GL); only a slight increase in mean liposome size was observed following gentamicin loading, round 200 nm in diameter. However, PDI and Zeta-potential were fairly similar to drug-free liposome formulations; InvA497-functionalized (I-L) and non-modified (L), serving as controls. Treatment with gentamicin-loaded InvA497-functionalized liposomes (I-GL) was seen to result in a 30% reduction in infection load – a result which was significantly higher than that following treatment with other control formulations (Figure 7). This indicates the ability of such bacteriomimetic delivery system to facilitate successful internalization and subsequent intracellular activity of an anti-infective drug, otherwise unable to cross the host cell membrane,

4. Conclusion

In conclusion, the present study reports on surface functionalization of liposomes with a bacteria-derived invasion protein, InvA497, as a promising strategy for intracellular drug delivery. The successfully designed bioinvasive delivery system was shown to mimic InvA-expressing bacteria in its mechanism of cell adhesion and entry. As a proof of concept, InvA497-functionalized liposomes were loaded with gentamicin. Due to its poor permeability across cellular membranes, gentamicin is active against extracellular, but not against intracellular bacteria.[46] The incubation of such a formulation with epithelial cells, previously infected with *Y. pseudotuberculosis,* resulted in a significant reduction of intracellular bacteria. This result demonstrates the potential of InvA497-functionalized nanocarriers as a strategy to facilitate the intracellular delivery of anti-infective agents, opening new perspectives for the treatment of established intracellular infections by compounds otherwise incapable to reach such site of action. As an extension to the prototype described in this study, different bacterial adhesins of relevance in the infection process as well as different pharmacologically active ingredients could be investigated, opening new avenues to the field of drug delivery. For potential oral administration, additional technological measures are probably required, e.g. formulating these novel delivery systems in enteric-coated capsules,[47, 48]. As a further translational step, successful nanocarriers should be finally evaluated in vivo in the appropriate animal model.

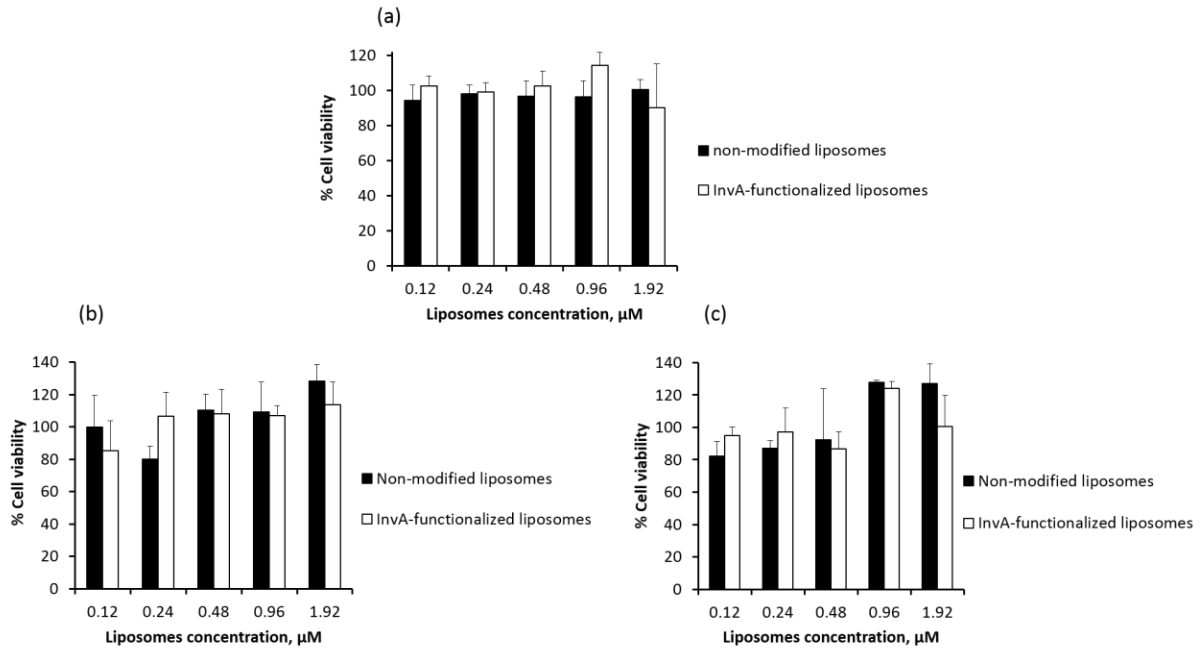

Figure 1. Viability of HEp-2 (a), non-polarized Caco-2 (b) and polarized Caco-2 cells (c) after incubation with non-modified or InvA497-functionalized liposomes at a concentration of 0.12-1.92 µM for 4 h (HEp-2 cells) or 8 h (Caco-2 cells).

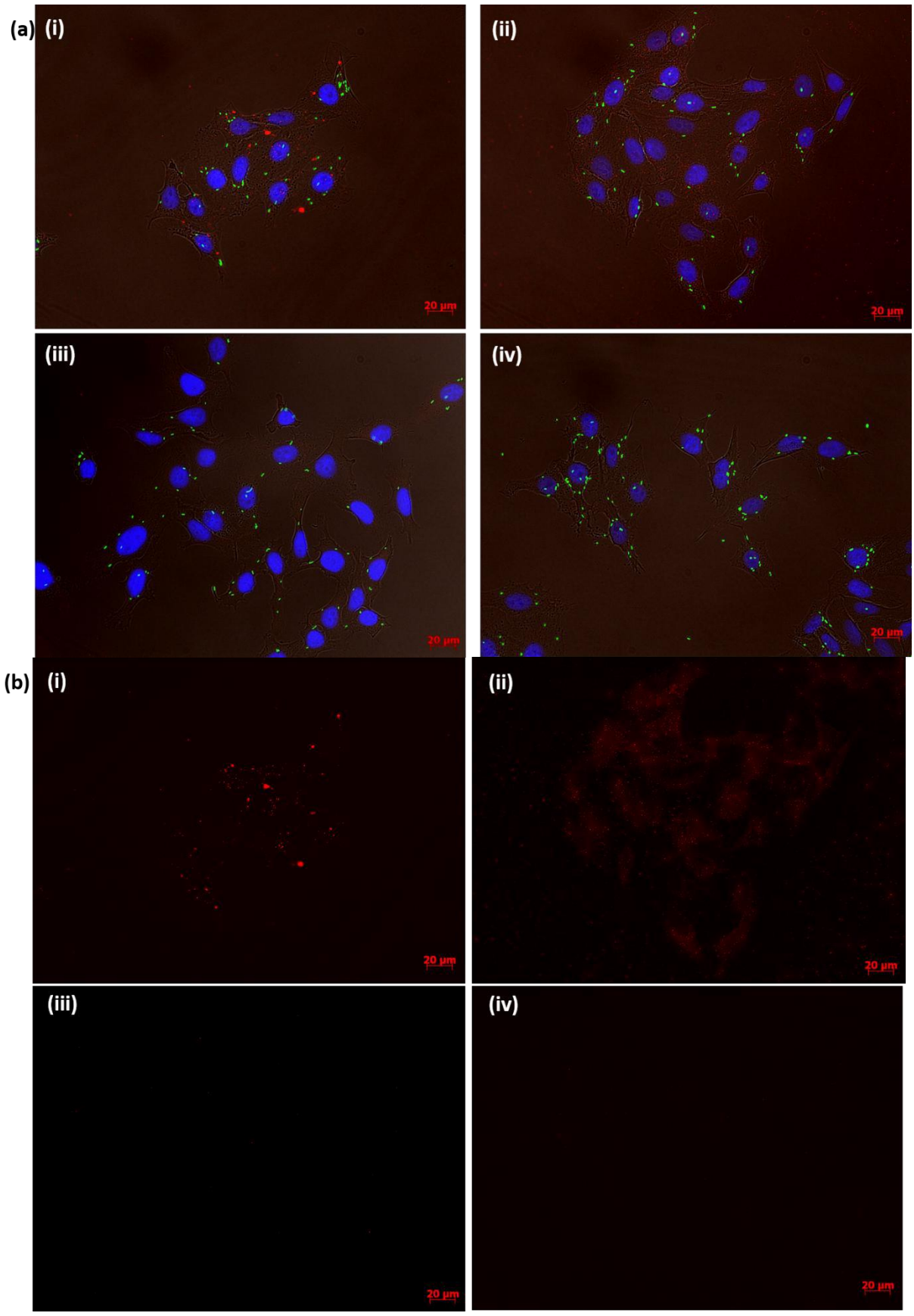
(a)
(i)
(ii)
(iii)
(iv)
(b)
(i)
(ii)
(iii)
(iv)
20 µm

(c)

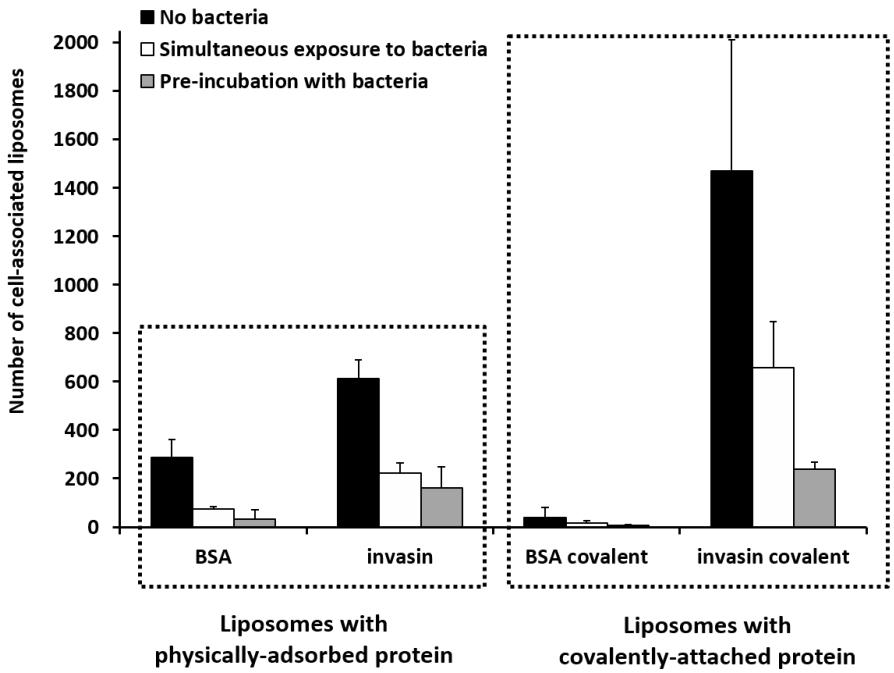

Figure 2. Adhesion of liposome formulations to HEp-2 cells in the presence or absence of InvA497- expressing *Yersinia pseudotuberculosis*. Representative overlaid fluorescence/transmission images (**a**) and the correspondent red channels (liposomes) (**b**), of 'late stage' infection simulation involving bacterial incubation followed by liposome addition, showing DAPI-stained nuclei (blue), GFP-expressing *Yersinia pseudotuberculosis* (green) and rhodamine-labelled liposomes (red). In each case, individual images represent exposure to liposomes with physically adsorbed InvA497 (i), covalently linked InvA497 (ii), physically adsorbed BSA (iii) and covalently linked BSA (iv). (C) Numbers of HEp-2 adherent liposomes in the absence of *Yersinia pseudotuberculosis*, with simultaneous exposure to bacteria and following pre-incubation with bacteria. Image analysis of fluorescence images (n = 5) expressed as weighed number of adhering liposomes per image field.

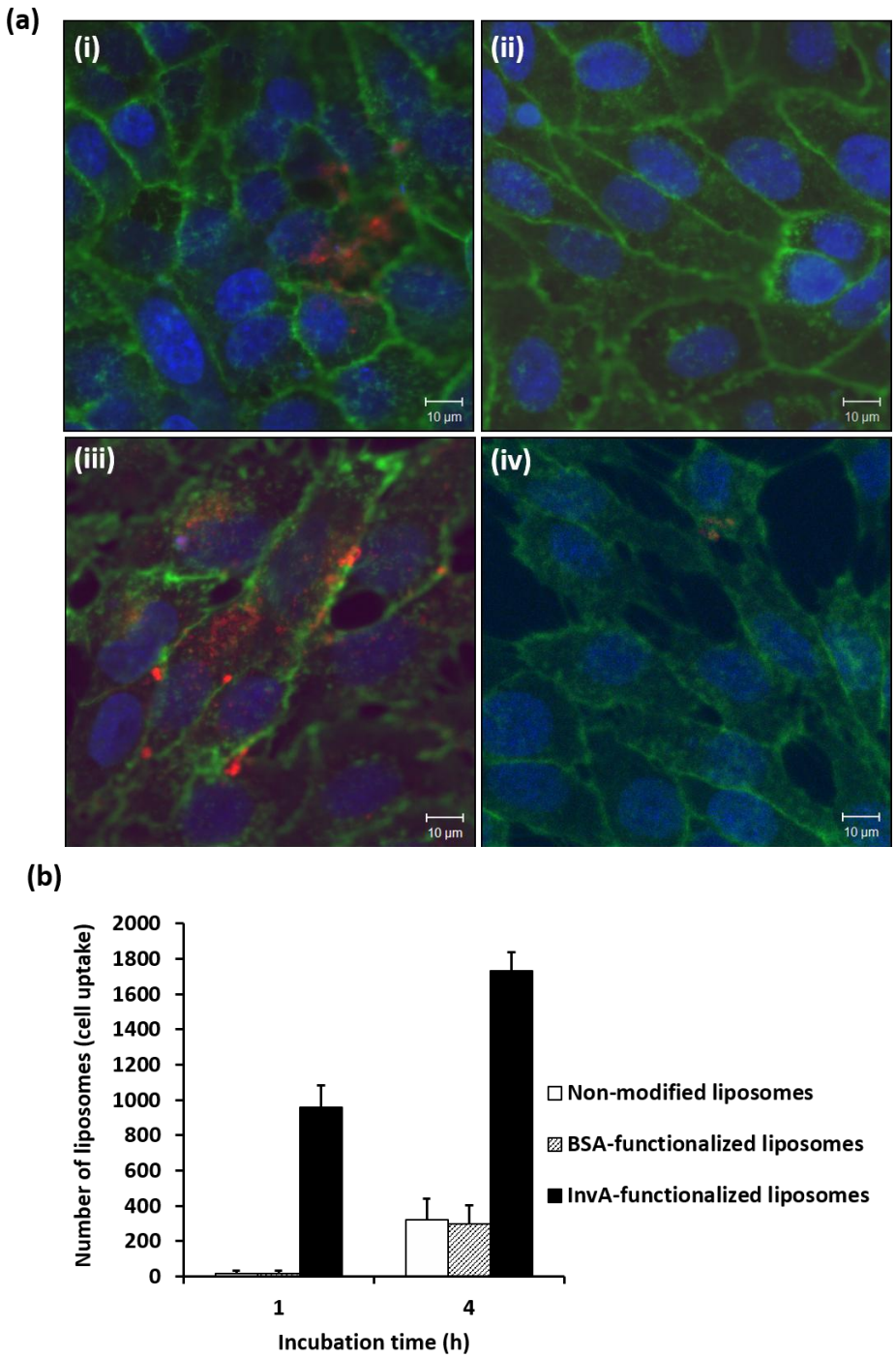

Figure 3. Analysis of relative uptake of liposomal formulations into HEp-2 cells. (a) Representative overlaid confocal-multiphoton images of HEp-2 cells incubated with InvA497-functionalized (i, iii) and non-modified (ii, iv) liposomes for 1 h (upper panel) and 4 h (lower panel), indicated as red spots. Indicated are DAPI-stained nuclei (blue), Flu-WGA-stained cell membranes (green) and rhodamine-labelled liposomes (red). (b) Image analysis of the z-projection images (developed by the freeware imageJ from the imaged z-stacks) of the red channel showing internalized liposomes expressed as weighed number of liposomes per z-stack (n = 3).

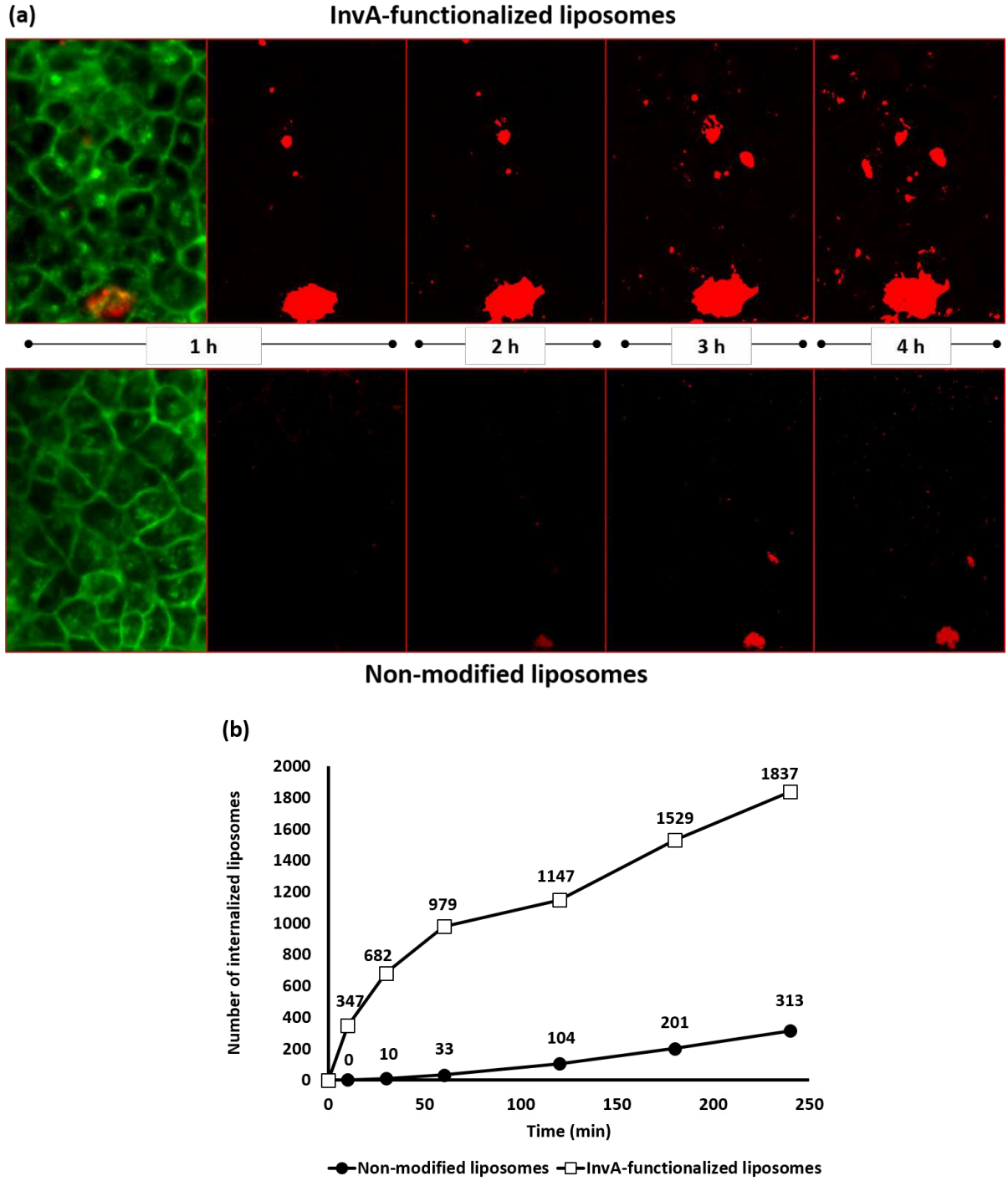

Figure 4. Kinetic analysis of liposomal uptake into HEp-2 cells. (a) Representative Z-projection images of the red channel of sequestered z-stacks of living HEp-2 cells incubated with InvA497-functionalized liposomes (upper panel) versus non-modified liposomes (lower panel) 1, 2, 3 and 4 h following liposome addition. Overlay images are presented for the first hour (far left image of each panel), additionally showing Flu-WGA-stained cell membranes in green. (b) Number of internalized InvA497-functionalized versus non-modified liposomes as a function of time.

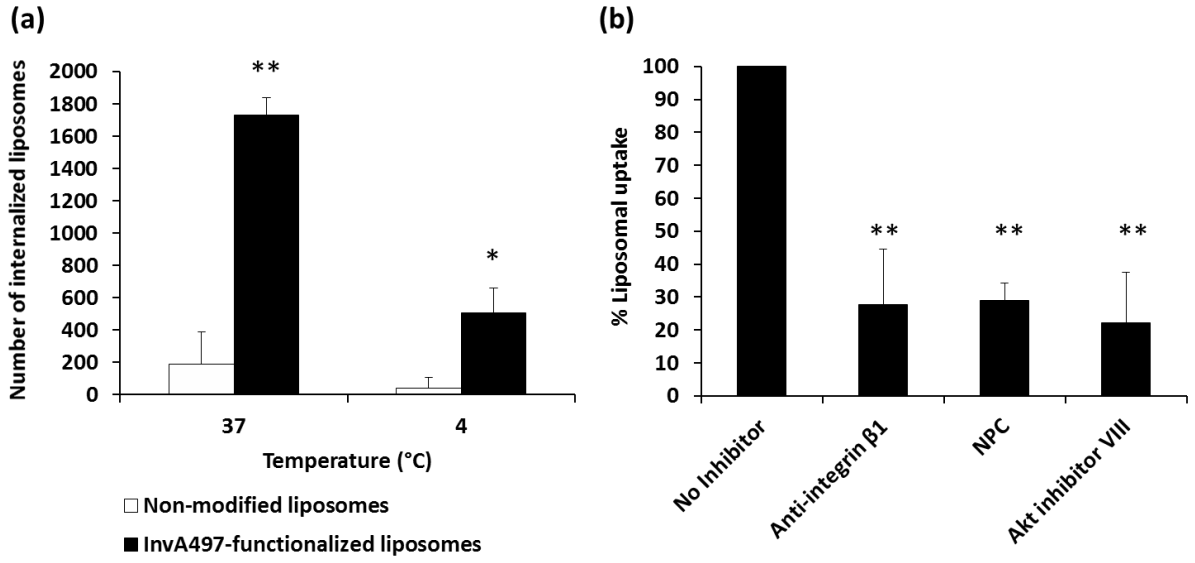

Figure 5. Mechanistic studies of liposomal uptake. One-way ANOVA with post-hoc Tukey test was used to demonstrate statistical significance. (a) Uptake of non-modified and InvA-functionalized liposomes at both 4 °C and 37 °C was investigated, in order to determine the energy-dependence of formulation uptake. Significant (p value < 0.05) and very significant (p value < 0.01) differences from the control non-modified liposomes at 37 °C were indicated in figure as * and **, respectively. (b) Investigation of receptor-specific uptake of InvA497-functionalized liposomes by incubation of HEp-2 cells with anti-β_1-integrin antibody or the InvA uptake inhibitors NPC-15437 or Akt inhibitor VIII, prior to liposome addition relative to control experiment in absence of inhibitor, indicated on figure as "no inhibitor". Very significant difference (p value < 0.01) from the control experiment was indicated in figure as **.

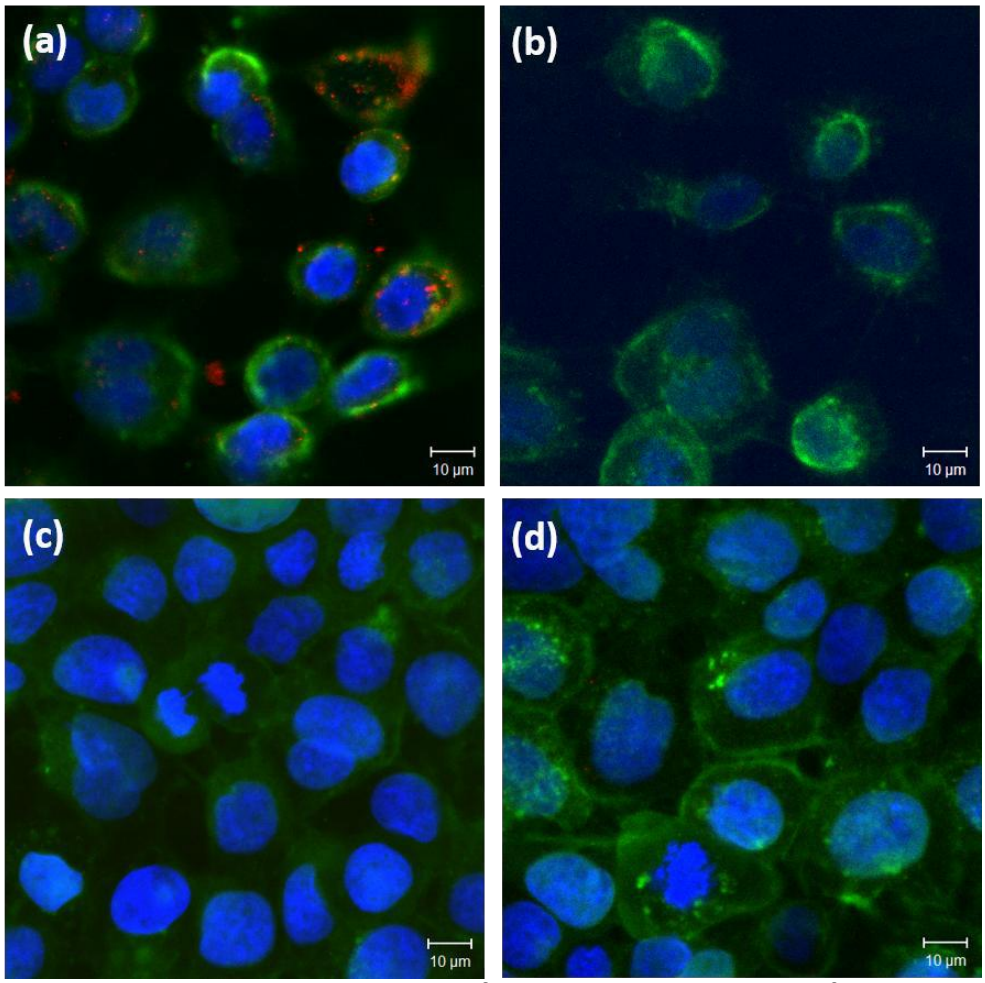

Figure 6. Representative overlaid confocal-multiphoton images of Caco-2 cells, approximately 50 % confluent (upper panel) and approximately 90 % confluent (lower panel) following incubation with InvA497-functionalized (a, c) and non-modified liposomes (b, d). DAPI-stained nuclei are indicated in blue, Flu-WGA-stained cell membranes are shown in green, and rhodamine-labelled liposomes are represented in red.

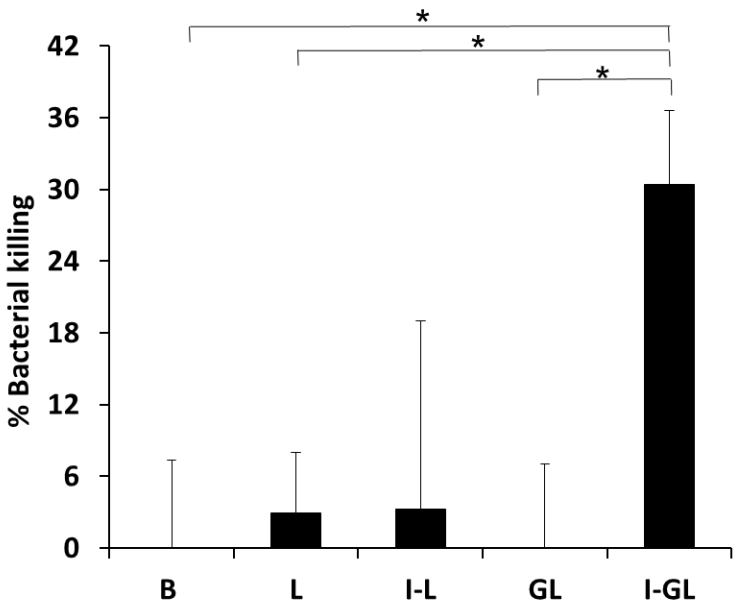

Figure 7. Anti-infective efficacy of liposome formulations. Killing percentage of *Yersinia pseudotuberculosis*-infected HEp-2 cells treated with different liposomal preparations: drug-free liposomes (L), InvA497-functionalized drug-free liposomes (I-L), gentamicin-loaded liposomes (GL) and InvA497-functionalized gentamicin-loaded liposomes (I-GL), and normalized to the untreated (blank, B). Significance was defined as * = p value < 0.05

Table 1. Physicochemical properties of prepared liposomes.

Liposomes	Size [nm]	Polydispersity index (PDI)	Zeta potential [mV]	Protein functionalization efficiency [%]	
				By BCA	By Western Blot
Non-modified	144.6 ± 1.7	0.03 ± 0.02	-19.9 ± 1.7	-	-
InvA497-functionalized	143.0 ± 0.4	0.05 ± 0.01	-25.5 ± 2.62	51.5 ± 4.5	50.0 ± 2.8
BSA- functionalized	140.6 ± 0.4	0.03 ± 0.01	-42.9 ± 0.6	43.3 ± 1.9	43.1 ± 2.9

Supporting Information:

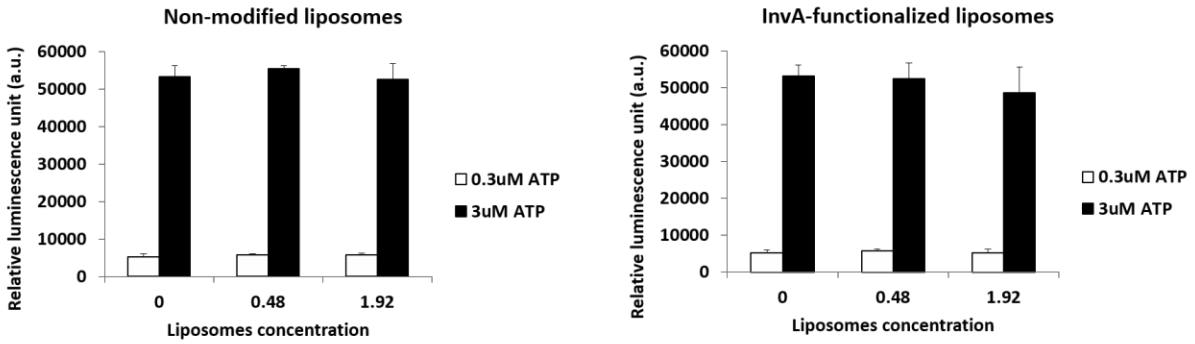

Figure S1: Interference testing of liposomes with (Vialight® Plus) viability kit in absence of cells. Luminescence measurement of ATP standards at 0.015 and 1.5 μM concentration in presence of non-modified (left Figure) and InvA497-functionalized (right Figure) liposomes was determined using (Vialight® Plus) viability kit reagent. No significant differences (*P*-value > 0.05) in luminescence values of both low and high ATP standards were observed at different liposomes concentration indicating lack of interference of liposomes with the assay reagent.

REFERENCES

[1] E. Haltner, J.H. Easson, C.M. Lehr, Lectins and bacterial invasion factors for controlling endo- and transcytosis of bioadhesive drug carrier systems, Eur J Pharm Biopharm, 44 (1997) 3-13.
[2] G. Ponchel, J.-M. Irache, Specific and non-specific bioadhesive particulate systems for oral delivery to the gastrointestinal tract, Adv Drug Deliv Rev, 34 (1998) 191-219.
[3] N. Hussain, A.T. Florence, Utilizing bacterial mechanisms of epithelial cell entry: invasin-induced oral uptake of latex nanoparticles, Pharm Res, 15 (1998) 153-156.
[4] G.F. Dawson, G.W. Halbert, The in vitro cell association of invasin coated polylactide-co-glycolide nanoparticles, Pharm Res, 17 (2000) 1420-1425.

[5] P. Dersch, R.R. Isberg, A region of the Yersinia pseudotuberculosis invasin protein enhances integrin-mediated uptake into mammalian cells and promotes self-association, EMBO J, 18 (1999) 1199-1213.
[6] P. Dersch, R.R. Isberg, An immunoglobulin superfamily-like domain unique to the Yersinia pseudotuberculosis invasin protein is required for stimulation of bacterial uptake via integrin receptors, Infect Immun, 68 (2000) 2930-2938.
[7] F. Uliczka, F. Pisano, J. Schaake, T. Stolz, M. Rohde, A. Fruth, E. Strauch, M. Skurnik, J. Batzilla, A. Rakin, J. Heesemann, P. Dersch, Unique cell adhesion and invasion properties of Yersinia enterocolitica O:3, the most frequent cause of human Yersiniosis, PLoS Pathog, 7 (2011) e1002117.
[8] Z.A. Hamburger, M.S. Brown, R.R. Isberg, P.J. Bjorkman, Crystal structure of invasin: a bacterial integrin-binding protein, Science, 286 (1999) 291-295.
[9] A. Wiedemann, S. Linder, G. Grassl, M. Albert, I. Autenrieth, M. Aepfelbacher, Yersinia enterocolitica invasin triggers phagocytosis via beta1 integrins, CDC42Hs and WASp in macrophages, Cell Microbiol, 3 (2001) 693-702.
[10] O.T. Buhler, C.A. Wiedig, Y. Schmid, G.A. Grassl, E. Bohn, I.B. Autenrieth, The Yersinia enterocolitica invasin protein promotes major histocompatibility complex class I- and class II-restricted T-cell responses, Infect Immun, 74 (2006) 4322-4329.
[11] S.E. Autenrieth, I.B. Autenrieth, Yersinia enterocolitica: subversion of adaptive immunity and implications for vaccine development, Int J Med Microbiol: IJMM, 298 (2008) 69-77.
[12] S. Anabousi, U. Bakowsky, M. Schneider, H. Huwer, C.M. Lehr, C. Ehrhardt, In vitro assessment of transferrin-conjugated liposomes as drug delivery systems for inhalation therapy of lung cancer, Eur J Pharm Sci, 29 (2006) 367-374.
[13] P.K. Smith, R.I. Krohn, G.T. Hermanson, A.K. Mallia, F.H. Gartner, M.D. Provenzano, E.K. Fujimoto, N.M. Goeke, B.J. Olson, D.C. Klenk, Measurement of protein using bicinchoninic acid, Anal Biochem, 150 (1985) 76-85.
[14] C. Schulze, U.F. Schaefer, C.A. Ruge, W. Wohlleben, C.-M. Lehr, Interaction of metal oxide nanoparticles with lung surfactant protein A, Eur J Pharm Biopharm, 77 (2011) 376-383.
[15] N. Nafee, M. Schneider, U.F. Schaefer, C.-M. Lehr, Relevance of the colloidal stability of chitosan/PLGA nanoparticles on their cytotoxicity profile, Int J Pharm, 381 (2009) 130-139.
[16] H.I. Labouta, T. Kraus, L.K. El-Khordagui, M. Schneider, Combined multiphoton imaging-pixel analysis for semiquantitation of skin penetration of gold nanoparticles, Int J Pharm, 413 (2011) 279-282.
[17] H.I. Labouta, L.K. el-Khordagui, T. Kraus, M. Schneider, Mechanism and determinants of nanoparticle penetration through human skin, Nanoscale, 3 (2011) 4989-4999.
[18] H.I. Labouta, L.K. El-Khordagui, T. Kraus, M. Schneider, Mechanism and determinants of nanoparticle penetration through human skin, Nanoscale, 3 (2011) 4989-4999.
[19] J. Gubernator, Z. Drulis-Kawa, A. Kozubek, A simply and sensitive fluorometric method for determination of gentamicin in liposomal suspensions, Int J Pharm, 327 (2006) 104-109.
[20] E. Harokopakis, G. Hajishengallis, S.M. Michalek, Effectiveness of liposomes possessing surface-linked recombinant B subunit of cholera toxin as an oral antigen delivery system, Infect Immun, 66 (1998) 4299-4304.
[21] T. Miyazaki, S. Yasumoto, Y. Kuzuya, T. Yoshimura, A primary study on oral vaccination with liposomes entrapping Koi Herpesvirus (KHV) antigens against KHV infection in Carp, in: M.G. Bondad-Reantaso, C.V. Mohan, M. Crumlish, R.P. Subasinghe (Eds.) Diseases in Asian

Aquaculture VI. Fish Health Section, Asian Fisheries Society, Manila, Philippines, 2008, pp. 99-184.
[22] J.V. Staros, R.W. Wright, D.M. Swingle, Enhancement by N-hydroxysulfosuccinimide of water-soluble carbodiimide-mediated coupling reactions, Anal Biochem, 156 (1986) 220-222.
[23] D. Sehgal, I.K. Vijay, A Method for the High Efficiency of Water-Soluble Carbodiimide-Mediated Amidation, Anal Biochem, 218 (1994) 87-91.
[24] Y. Gao, I. Kyratzis, Covalent Immobilization of Proteins on Carbon Nanotubes Using the Cross-Linker 1-Ethyl-3-(3-dimethylaminopropyl)carbodiimide—a Critical Assessment, Bioconjugate Chem, 19 (2008) 1945-1950.
[25] N. Lewinski, V. Colvin, R. Drezek, Cytotoxicity of nanoparticles, Small, 4 (2008) 26-49.
[26] K.J. Ong, T.J. MacCormack, R.J. Clark, J.D. Ede, V.A. Ortega, L.C. Felix, M.K.M. Dang, G. Ma, H. Fenniri, J.G.C. Veinot, G.G. Goss, Widespread Nanoparticle-Assay Interference: Implications for Nanotoxicity Testing, PLoS ONE, 9 (2014) e90650.
[27] B. Wahl, N. Daum, H.-L. Ohrem, C.-M. Lehr, Novel luminescence assay offers new possibilities for the risk assessment of silica nanoparticles, Nanotoxicology, 2 (2008) 243-251.
[28] A.A. Spector, M.A. Yorek, Membrane lipid composition and cellular function, J Lipid Res, 26 (1985) 1015-1035.
[29] B.S. Zolnik, A. González-Fernández, N. Sadrieh, M.A. Dobrovolskaia, Minireview: Nanoparticles and the Immune System, Endocrinology, 151 (2010) 458-465.
[30] A. Arjonen, J. Alanko, S. Veltel, J. Ivaska, Distinct Recycling of Active and Inactive β1 Integrins, Traffic (Copenhagen, Denmark), 13 (2012) 610-625.
[31] K. Rege, I.L. Medintz, Methods in Bioengineering: Nanoscale Bioengineering and Nanomedicine, in, Artech House, 2014, pp. 365 pages.
[32] J. Eitel, P. Dersch, The YadA protein of Yersinia pseudotuberculosis mediates high-efficiency uptake into human cells under environmental conditions in which invasin is repressed, Infect Immun, 70 (2002) 4880-4891.
[33] T.T. Nguyen, J.L. Swift, M.C. Burger, D.T. Cramb, Effects of Various Small-Molecule Anesthetics on Vesicle Fusion: A Study Using Two-Photon Fluorescence Cross-Correlation Spectroscopy, J Phys Chem B, 113 (2009) 10357-10366.
[34] P. de Diesbach, F. N'Kuli, C. Berens, E. Sonveaux, M. Monsigny, A.C. Roche, P.J. Courtoy, Receptor-mediated endocytosis of phosphodiester oligonucleotides in the HepG2 cell line: evidence for non-conventional intracellular trafficking, Nucleic acids research, 30 (2002) 1512-1521.
[35] H. Herd, N. Daum, A.T. Jones, H. Huwer, H. Ghandehari, C.-M. Lehr, Nanoparticle Geometry and Surface Orientation Influence Mode of Cellular Uptake, ACS Nano, 7 (2013) 1961-1973.
[36] F. Uliczka, T. Kornprobst, J. Eitel, D. Schneider, P. Dersch, Cell invasion of Yersinia pseudotuberculosis by invasin and YadA requires protein kinase C, phospholipase C-gamma1 and Akt kinase, Cell Microbiol, 11 (2009) 1782-1801.
[37] A. Marra, R.R. Isberg, Analysis of the Role of Invasin during Yersinia pseudotuberculosis Infection of Mice, Ann NY Acad Sci, 797 (1996) 290-292.
[38] J.F. Beaulieu, Differential expression of the VLA family of integrins along the crypt-villus axis in the human small intestine, J Cell Sci, 102 (1992) 427-436.
[39] K.L. Edelblum, J.R. Turner, The tight junction in inflammatory disease: communication breakdown, Curr Opin Pharmacol, 9 (2009) 715-720.
[40] J. Susewind, C. de Souza Carvalho-Wodarz, U. Repnik, E.-M. Collnot, N. Schneider-Daum,
G.W. Griffiths, C.-M. Lehr, A 3D co-culture of three human cell lines to model the inflamed intestinal mucosa for safety testing of nanomaterials, Nanotoxicology, (2015) 1-10.
[41] F. Leonard, E.M. Collnot, C.M. Lehr, A three-dimensional coculture of enterocytes,

monocytes and dendritic cells to model inflamed intestinal mucosa in vitro, Mol Pharmaceutics, 7 (2010) 2103-2119.
[42] M.-H. Coconnier, M.-F. Bernet-Camard, A.L. Servin, How intestinal epithelial cell differentiation inhibits the cell-entry of Yersinia pseudotuberculosis in colon carcinoma Caco-2 cell line in culture, Differentiation, 58 (1994) 87-94.
[43] J.H. Brumell, P. Tang, M.L. Zaharik, B.B. Finlay, Disruption of the Salmonella-containing vacuole leads to increased replication of Salmonella enterica serovar typhimurium in the cytosol of epithelial cells, Infect Immun, 70 (2002) 3264-3270.
[44] S. Mostowy, P. Cossart, Bacterial autophagy: restriction or promotion of bacterial replication?, Trends in cell biology, 22 (2012) 283-291.
[45] O.L. Champion, A. Karlyshev, I.A. Cooper, D.C. Ford, B.W. Wren, M. Duffield, P.C. Oyston, R.W. Titball, Yersinia pseudotuberculosis mntH functions in intracellular manganese accumulation, which is essential for virulence and survival in cells expressing functional Nramp1, Microbiology, 157 (2011) 1115-1122.
[46] C. Kumana, K. Yuen, Parenteral Aminoglycoside Therapy, Drugs, 47 (1994) 902-913.
[47] S. Hua, Orally administered liposomal formulations for colon targeted drug delivery, Front in Pharmacol, 5 (2014) 138.
[48] A.S. Gupta, S.J. Kshirsagar, M.R. Bhalekar, T. Saldanha, Design and development of liposomes for colon targeted drug delivery, J Drug Targeting, 21 (2013) 146-160.